

## A new and powerful approach to mapping large-scale landslides using InSAR and LiDAR derived DEMs

Chih-Yao Yang<sup>1</sup>, C.-Y. Chi<sup>1</sup>, R.-F. Chen<sup>2</sup>, and C.-W. Lin<sup>3</sup>

<sup>1</sup>CECI Engineering Consultants, Inc., NO.323, Yangguang St., Neihu District, Taipei City 11491, Taiwan (R.O.C.)

<sup>2</sup> Department of Geology, Chinese Culture University, 55, Hwa-Kang Road, Yang-Ming-Shan, Taipei City 11114, Taiwan (R.O.C.)

<sup>3</sup> Department of Earth Sciences, National Cheng Kung University, No.1, University Road, Tainan City 701, Taiwan (R.O.C.)

### ABSTRACT

In recent years, natural disasters occurred more frequently than before mainly due to extreme rainfall arising from global climate change. The Hsiaolin landslide that caused 450 casualties during the 2009 Typhoon Morakot is a typical example known to many people.

After Hsiaolin Landslide, Central Geological Survey and Soil and water Conservation Bureau have devoted great efforts to map potential large-scale landslides using LiDAR-derived 1 m DEM. So far, over ten thousands of large-scale landslides have been identified. Considering vulnerability and risks involved, 182 deep-seated landslides have been selected for further landslide hazard mitigation. Additionally, InSAR analysis that can provide mm resolution displacement rate is also employed to help to determine which site needs to be paid more attention with.

This paper has selected Dingyuan New Village in Nantou County to illustrate how to use both of LiDAR derived DEMs and the results of Temporarily Coherent Point SAR Interferometry (TCP-InSAR) to locate large-scale landslides.

**Keywords:** large-scale landslides; InSAR; LiDAR derived DEMs

### 1 INTRODUCTION

Over the last two decades, the developments of Light Detection And Ranging (LiDAR) derived Digital Terrain Model (DTM) and Interferometric Synthetic Aperture Radar (InSAR) have been two important breakthroughs in the studies of slope disasters around the world. LiDAR derived DTM can reflect topographic features of actual terrain and locate moving blocks through interpretive analysis, whereas InSAR provides millimeter accurate deformation data. In the past, InSAR has not been widely applied due to high costs of purchasing digital images and a relatively higher threshold for data analysis and operations derived therefrom. Nevertheless, following the open and free access of satellite images in recent years, this technique has been rapidly developed. The exponential progress of computing hardware also facilitated the applications of InSAR technique, enabling the scholars and experts to acquire large-scale deformation data of and to evaluate the activity of potential large-scale landslides.

As highly-developed slopes can lose their original topographic features and result in difficulties in identifying landslide signatures using LiDAR, this paper aims to explain the possibility of using InSAR analysis results to fix or adjust the boundaries of potential large-scale landslides; and to prove that the

combination of LiDAR and InSAR techniques enables us to even more precisely evaluate the range and scale of disaster impacts. By taking Dingyuan New Village as an example, two landslide prone areas (sites D057-Renai-Nantou and No. D063-Renai -Nantou) were originally interpreted. However, according to the results of time-series deformation analysis conducted by TCPInSAR and landslide failure mechanisms identified there from, these two sites actually have identical sliding pattern and are therefore integrated as one large-scale landslide for future investigation and preventive works.

### 2 RESEARCH METHODS

This study aims to interpret and adjust the range and scale of potential large-scale landslide by integrating InSAR, which can evaluate the landslide activity, and LiDAR, which can identify and interpret topographic features of landslide, techniques.

#### 2.1 Calculation of ground surface deformation using satellite radar images

InSAR uses radar echo signals to receive the 3D information of ground surface and Differential Synthetic Aperture Radar Interferometry (DInSAR), for example, enables us to measure crustal deformation. The concept of DInSAR is to calculate the interference pattern of two satellite images acquired in different

time over the same area after geometric corrections; perform the atmospheric, orbit, and topographic correction steps to calculate the phase (travel time) difference of radar echoes between the ground surface and satellite; and then convert the interferometric phase into Line-Of-Sight (LOS) to acquire high-precision terrain deformation (Fig. 1).

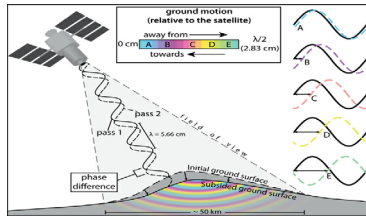


Fig. 1. A cartoon representation of the basic principles of radar interferometry (Source: Global Volcanism Program, 2012).

Ferretti et al. (2001) proposed the Permanent Scatterers Interferometry (PSInSAR) technique to effectively correct atmospheric effects, phase difference and topographic errors, issues that are often seen in conventional interferograms. The PSInSAR technique searches for persistent scatterer (PS) with high correlation over a long period of time from SAR images acquired at different time.

The scatterers, which provide good phase information, can overcome the challenges of SAR images with respect to time and space. It also enhances the calculation precision of PSInSAR and make the phase information more reliable relatively (Fig. 2). In recent years, PSInSAR has been widely applied in slow-moving ground surface deformation, such as coseismic deformation, subsidence and ground service deformation over a long period of time (Hooper et al., 2007; Yen et al., 2010; Yan, 2011; Su, 2012). The principal advantages of PSInSAR are: (1) High accuracy with respect to baseline; (2) can effectively overcome atmospheric factors; (3) displacement of scatterers with high spatial density; (4) facilitation of long-term monitoring.

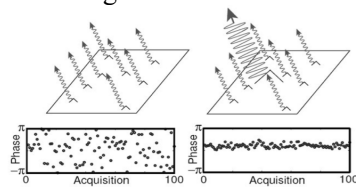


Fig. 2. Illustration of the principle of PSInSAR (Hooper et al., 2007)

Nevertheless, comparing cities that have well-developed infrastructure, mountain areas that feature rough terrain and dense vegetation provide relatively less information due to limited number of stable scatterers. Zhang (2011) therefore proposed the Temporarily Coherence Point InSAR (TCPIInSAR) technique to, with the use of phase difference of PS, do generalized least squares and classify PS based on their

ambiguity by identify the size of residuals. With the use of this technique, the phase unwrapping process, in which errors and failure often occur, can therefore be replaced to further calculate the ground deformation rate (Fig. 3). At the current stage, this technique has already been applied in the studies of deep-seated landslides in Lushan and Cingjing of Taiwan; the results thereof conform to the the high-precision DTM interpretation results and field investigation, proving that this technique is ideal for highly vegetated mountainous areas in Taiwan.

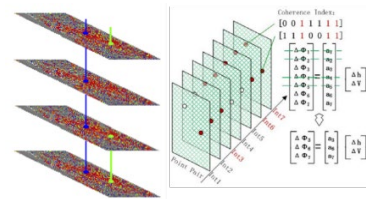


Fig. 3. Illustration of the TCPIInSAR Technique (Modified from Zhang et al., 2011).

## 2.2 Identification of landslide topographic features from LiDAR derived DTM

Satellite imagery, aerial photos and high-precision DTM data were also collected in this study to not only identify detailed topographic features of landslide areas, but also understand the evolutionary development of deep-seated landslides and locate subsiding areas therewithin. The reason for adopting this multiple approach is that the scale of deep-seated landslides is enormous and there are usually a number of subsiding areas at different activity level therewithin. Furthermore, field investigations are often challenged by rough terrain and transportation, making it difficult to reach the destination or investigate the entire scope in details. Therefore, before conducting a field investigation, a detailed interpretation of the landslide imagery is required to better understand the topographic features and surrounding environment thereof (as illustrated in Fig. 4). This step is therefore rather important as it not only facilitates field investigation with detailed information, but also enables the scholars and experts to estimate the landslide mechanism of deep-seated landslide.

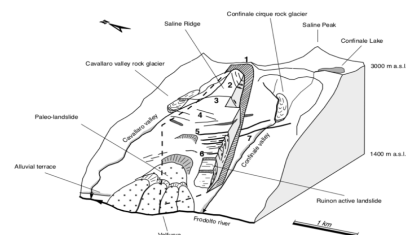


Fig. 4. Illustration of topographic features of deep-seated landslides (Agliardi, et al., 2001)

Landslide failure mechanisms, which are are Interpreted based on detailed topographic features of

the landslide area and the environment of its surrounding areas, can be used not only to conduct disaster prevention and mitigation works, but also to evaluate the landslide activity. The landslide failure mechanism can be mainly classified as follows:

(1) Drainage characteristics

Surface crack and bedrock fracture are important channels through which the surface water infiltrate into the bedrock. If the landslide slope has a well-developed drainage system comparing with the surrounding area or the drainage system is close thereto, it means that the slope is likely to become a gully due to the erosion effects of surface water; and that the scope of bedrock exposure or surface crack will further expand. With respect to landslide areas, the distribution of the drainage system can tell the erosion resistance level of the region's surface material; the development of landslide topography; and level of bedrock erosion induced by surface water.

(2) Interpretation of deep-seated landslide signatures

The interpretation is focused on the landslide signatures, including the main scarp, minor scarp, lateral scarp, cracks and the distribution of multiple ridge. As minor scarps, commonly known as subsiding areas, often occur in a deep-seated landslide (Lin, et al., 2013), identified minor scarps are often classified according to their arrangement and type: The primary minor scarp is the sliding surface closest to the main scarp, whereas the secondary and tertiary minor scarps refer to the sliding surface formed therewithin as illustrated in Fig. 4.

(3) Subsiding areas and blocks of deep-seated landslide

The enormous deep-seated landslide is often formed by a number of subsiding blocks. Therefore, in the interpretation of deep-seated landslide, scarp location and continuity are often evaluated together with the location of flat surface and characteristics of drainage system to outline subsiding blocks.

(4) Topographic environment of surrounding areas

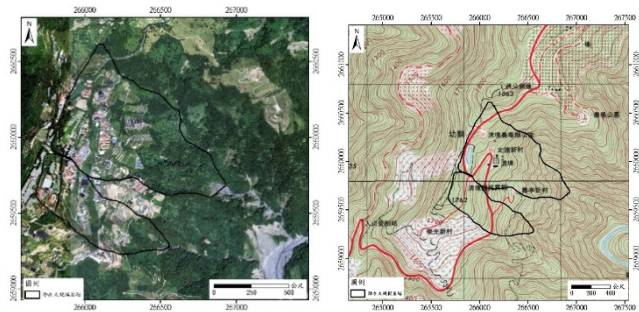
The objective of interpreting landslide surrounding areas is to better understand how the deep-seated landslide is related to its surrounding environment. Such interpretation enables us to have a rough idea on the potential external landslide triggering factors and whether the toe is protected by the stream terrace as illustrated in Fig. 4. The interpretation items include the location of bank erosion, alluvium and stream terrace.

### 3 CASE STUDIES

#### 3.1 LiDAR derived DTM interpretation results

The study area is Dingyuan New Village of Renai Village in Nantou County (Fig. 5a). There is no obvious

shallow landslide in surrounding areas. The upper slope is an agricultural land, whereas the lower slope is a primary forest (as illustrated in Fig. 5b (photo taken on September 9, 2009 after Typhoon D057Morakot). As the original topographic features of this area is covered by dense vegetation and damaged by human activities, it is hard to identify the signatures and location of deep-seated landslide using only satellite images and aerial



photos

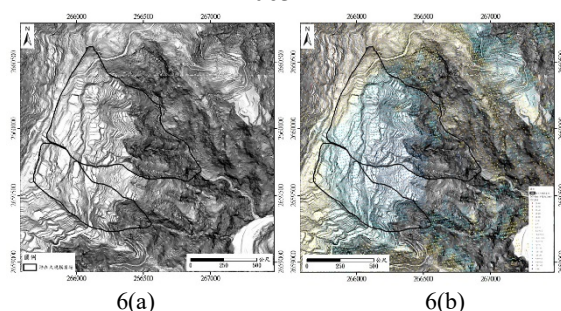
5(a)

5(b)

Fig. 5(a). Deep-seated landslide mapping before the adjustment.

(b). Deep-seated landslide mapping after the adjustment.

LiDAR derived DEM, which has been widely and successfully used to interpret deep-seated landslides in recent years, has advantages of mapping actual topography and providing high resolution data. Nevertheless, in areas where the original topography and scarp continuity are damaged by human activities, the interpretation of deep-seated landslide becomes difficult. In this study, a LiDAR derived DTM based analysis is adopted for identifying deep-seated landslides in the region. In the study area, the ridge in the middle of the slope was damaged by human activities and therefore makes the arched scarp unnoticeable, and gives an illusion that this area is relatively stable. With the use of high-precision LiDAR derived DTM, two deep-seated landslides, sites D057-Renai-Nantou and No. D063-Renai -Nantou.



6(a)

6(b)

Fig. 6(a). LiDAR derived DTM of D057 and D063 before the adjustment.(b). Distribution of the coherence points of deep-seated landslide before the adjustment.

#### 3.2 TCPIInSAR interpretation results

The ALOS satellite imagery was also adopted to calculate the slope deformation of study area using TCPIInSAR. Between 2006 and 2011, the ridge of surrounding areas and the ridge located on the landslide



boundary uplifted, whereas the ridge on the slope and the surface displacement of landslide areas subsided, indicating that sites D057 and D063 have the same displacement pattern(Fig. 6b).

### 3.3 LiDAR derived DEM and InSAR interpretation results

With respect to highly cultivated areas or areas with difficulties in interpretation, the use of LiDAR derived DTM and InSAR imagery provides us not only the information on landslide micro-topography, but also the long-term deformation. This enables us to understand the slope stability and land subsidence, and further determine the range of deep-seated landslide and make adjustments thereto (Fig. 7a).

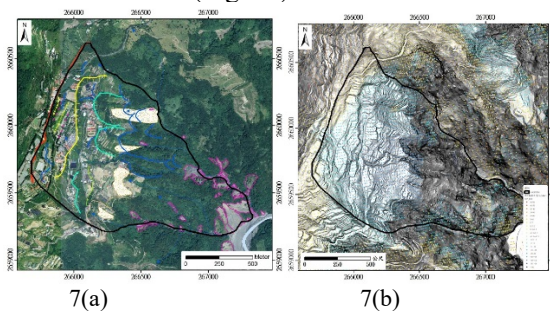


Fig. 7. Distribution of the coherence points of deep-seated landslide after the adjustment and the landslide signatures (a) aerial photos(b) LiDAR

LiDAR derived DEM and InSAR imagery were adopted in this study(Fig. 7b). The results revealed that, although a number of scarps sites D057 and D063 were damaged by human activities, their surrounding areas actually shared the same displacement pattern according to the InSAR analysis. As this infers the slope of where Dingyuan New Village is located is a part of deep-seated landslide, an amendment was made to the mapping thereto.

## 4 CONCLUSION

With respect to the interpretation of deep-seated landslide, using merely landslide micro-topography is hard to determine the boundaries of deep-seated landslides particularly in highly cultivated areas or areas with difficulties in interpretation. An approach associated with InSAR imagery can, on the other hand, facilitate and ameliorate the mapping of sliding surfaces; and provide detailed and accurate information for future investigations and disaster mitigation works.

## REFERENCES

- Agliardi, F., Crosta, G., & Zanchi, A. (2001). Structural constraints on deep-seated slope deformation kinematics. *Engineering Geology*, 59(1-2), 83-102.
- Amelung, F., Jónsson, S., Zebker, H., & Segall, P. (2000). Widespread uplift and 'trapdoor' faulting on Galapagos volcanoes observed with radar interferometry. *Nature*, 407(6807), 993.
- Ferretti, A., Prati, C., & Rocca, F. (2001). Permanent scatterers in SAR interferometry. *IEEE Transactions on geoscience and remote sensing*, 39(1), 8-20.
- Hoffmann, J., Galloway, D. L., & Zebker, H. A. (2003). Inverse modeling of interbed storage parameters using land subsidence observations, Antelope Valley, California. *Water Resources Research*, 39(2).
- Hooper, A., Segall, P., & Zebker, H. (2007). Persistent scatterer interferometric synthetic aperture radar for crustal deformation analysis, with application to Volcán Alcedo, Galápagos. *Journal of Geophysical Research: Solid Earth*, 112(B7).
- Hung, W.C., Hwang, C.W., & Chung, C.P. (2010). Using Leveling, GPS, Subsidence Monitoring Well and D-InSAR to Monitor the Subsidence in Yunlin Region. Technical Paper in the Land Subsidence Database, WRA, Taiwan.
- Lin, C. W., Tseng, C. M., Tseng, Y. H., Fei, L. Y., Hsieh, Y. C., & Tarolli, P. (2013). Recognition of large scale deep-seated landslides in forest areas of Taiwan using high resolution topography. *Journal of Asian Earth Sciences*, 62, 389-400.
- Massonnet, D., Adragna, F., & Rossi, M. (1994). CNES general-purpose SAR correlator. *IEEE transactions on geoscience and remote sensing*, 32(3), 636-643.
- Pathier, E., Fruneau, B., Deffontaines, B., Angelier, J., Chang, C. P., Yu, S. B., & Lee, C. T. (2003). Coseismic displacements of the footwall of the Chelungpu fault caused by the 1999, Taiwan, Chi-Chi earthquake from InSAR and GPS data. *Earth and Planetary Science Letters*, 212(1-2), 73-88.
- Su, P. T. (2012). A PSInSAR Method with Redundant Observations. National Cheng Kung University Department of Geomatics Master's Thesis, 1-96.
- Varnes, D. J. (1978). Slope Movement Types and Processes.[In:] Schuster RL & Krizek RJ (eds), *Landslides: Analysis and Control*. Special Rep. 176. Transportation Research Board, Nat. Acad. of Science, Washington.
- Yang, J. S. (2011). An Improved PS-InSAR Approach. National Cheng Kung University Department of Geomatics Master's Thesis, 1-169.
- Yen, J. Y., Lu, C. H., Chang, C. P., Hooper, A. J., Chang, Y. H., Liang, W. T., Chang, T. Y., Lin, M. S., & Chen, K. S. (2010). Investigating the active deformation in the northern Longitudinal Valley and Hualien City of eastern Taiwan by using Persistent Scattered and Small-baseline SAR Interferometry *Terrestrial Atmospheric and Oceanic Sciences*, 22(3):291-304.
- Zhang, L., Ding, X., & Lu, Z. (2011). Ground settlement monitoring based on temporarily coherent points between two SAR acquisitions. *ISPRS Journal of Photogrammetry and Remote Sensing*, 66(1), 146-152.
- Zhang, L., Ding, X. L., & Lu, Z. (2011, September). Deformation rate estimation on changing landscapes using temporarily coherent point InSAR. In *Proc. Fringe* (pp. 19-23)